Nonlinear Physical Optics With Transversely Patterned Quasi-Phase-Matching Gratings

Jonathan R. Kurz, Andrew M. Schober, David S. Hum, A. J. Saltzman, and Martin M. Fejer, *Member, IEEE*

***Abstract*—Transverse patterning of periodic gratings for quasi-phase-matching (QPM) at the micron scale leads to a multitude of nonlinear optical devices based on familiar physical optics effects. We demonstrate spatial control over the amplitude and phase of a second-harmonic beam in multiple slit diffraction devices and in QPM lenses, which are nonreciprocal devices.**

***Index Terms*—Diffraction, nonlinear optical devices, nonreciprocity, periodically poled lithium niobate, physical optics, quasi-phase-matching.**

I. Introduction

TRANSVERSE patterning of periodic gratings for quasi–phase-matching (QPM) has been used to increase the tuning range of devices (through fanned gratings) [1], to shape the amplitude profile of an interacting beam [2], and to create two-dimensional periodic QPM structures (nonlinear photonic crystals) [3], [4] for efficient noncollinear mixing. Devices with micron-scale transverse control of the position and width—as measured perpendicular to the k vector—of individual grating segments can also be viewed as a programmable amplitude and phase mask for nonlinear mixing. Narrow stripes of precisely positioned grating can be treated as coherent optical line sources suitable for demonstrating a multitude of one-dimensional (1-D) physical optics effects. In the far field, these line sources can be treated as 1-D "slit" sources. We present some familiar effects from physical optics, including diffraction from single and multiple slits, that demonstrate spatial control of amplitude and phase using transversely patterned QPM.

The analogy between a transversely patterned QPM source and 1-D diffraction at a hard aperture is illustrated in Fig. 1. With the proper arrangement of inverted domains, the QPM gratings—which have no effect on the first-harmonic (FH) wave in the undepleted pump approximation—form controllable slits for the second harmonic (SH) output. This analogy holds when the length of the gratings is short compared to the Rayleigh range of the SH output from the narrowest slits so that diffraction within the device can be ignored. In devices with multiple slits, the relative phase of every slit can be independently adjusted with high precision from 0 to 2π radians by shifting the position of the entire grating stripe by a fraction of a QPM grating period (Λ_g). In Fig. 1, a shift of distance (d) in the third grating adjusts its relative phase ($\phi = 2\pi d/\Lambda_g$) and modulates the position of intensity peaks in the far field. Using an array of phase-shifted grating stripes, it is possible to approximate an arbitrary phase profile across a beam in discrete steps that are limited by the minimum grating width and spacing. This technique enables the design and fabrication of more complicated structures such as QPM lenses.

Manuscript received February 12, 2002; revised March 21, 2002. This work was supported by DARPA through the Optoelectronics Materials Research Center (Prime MDA972-00-1-0024), the U.S. Air Force Office of Scientific Research (Grant F49620-99-1-0270), the Center for Novel Electronic Devices Industrial Affiliates Program, the Stanford Photonics Research Center, the Stanford Optical Signal Processing Collaboration, the Stanford Graduate Fellowships Program, and Crystal Technologies, Inc.

The authors are with the E. L. Ginzton Laboratory, Stanford University, Stanford, CA 94305 USA.

Publisher Item Identifier S 1077-260X(02)05466-7.

II. QPM Physical Optics Devices

A. Fabrication

We fabricated a variety of single, double, and multiple grating stripe patterns in periodically poled lithium niobate (PPLN) by electric-field-poling of whole wafers (z cut, 0.5 mm thick) [5]. In the poling process, a liquid electrolyte was used to contact the wafer through a photoresist electrode pattern. Fig. 2 shows grating stripes and arrays (revealed by etching in hydrofluoric acid) that range in width from 8 to 50 μm with an 18.6-μm period. In this figure, the accurate slit widths and Fresnel zone plate pattern reveal good transverse control over domain size and position, while the displaced slit pair and parabolic phase array demonstrate fine control over grating phase shifts. Fresnel phase plates, made from two complementary Fresnel amplitude plates with a π-phase shift, were also created.

Arrays of inverted domains as small as 8 μm in size (with 8 μm edge-to-edge spacing) were poled with few defects—less than 0.1% of the domains were missing or merged. Smaller feature sizes enhance nucleation because of high fringing fields at the electrode edges. Consequently, for a given QPM period, fine transverse patterning *improves* poling fidelity, resulting in more uniformly sized domains with straighter edges. At the same time, increasing the duty cycle of the transverse patterning seems to suppress nucleation, limiting the pattern density. Domains grow in hexagonal structures due to the crystalline symmetry of congruent lithium niobate, and the resulting 60° corners on each inverted domain may slightly apodize the transverse patterning. Improvements to the periodic poling technique that reduce the minimum transverse grating period will help realize the full potential of QPM physical optics structures.

B. Single, Double, and Multiple Slit Diffraction Devices

To demonstrate classic Fraunhofer diffraction, we measured second-harmonic generation (SHG) of 1.55-μm light in the transversely patterned QPM devices. After dicing and end-face polishing, devices were tested using 100-fs pulses from a synchronously pumped optical parametric oscillator (OPO) system

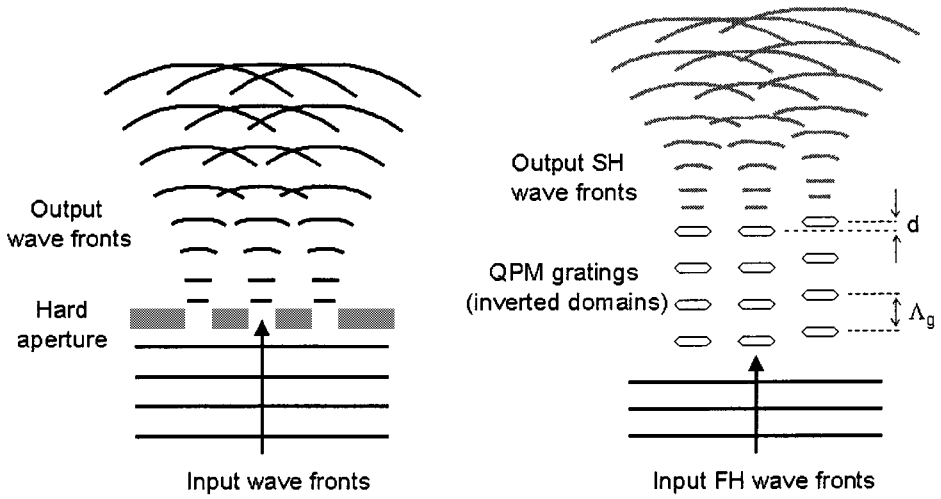

Fig. 1. The analogy between a transversely patterned QPM source and 1-D diffraction at a hard aperture.

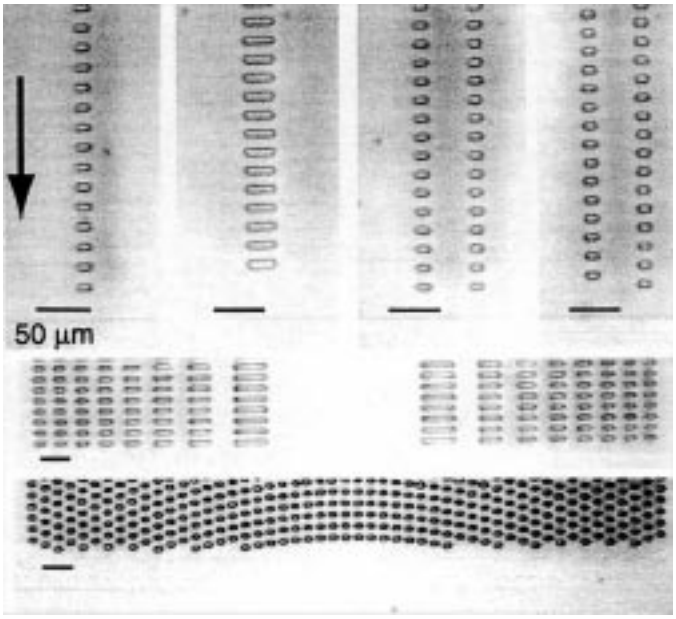

Fig. 2. QPM nonlinear physical optics structures in etched PPLN. Top row from left: Single slit devices (10 μm and 25 μm widths); double slits (10 μm width and 50 μm spacing) with zero and π relative phase shifts. Bottom: A Fresnel zone plate structure and a parabolic phase array of 8-μm-wide domains. The arrow indicates propagation direction, while the scale bar indicates 50 μm in each image.

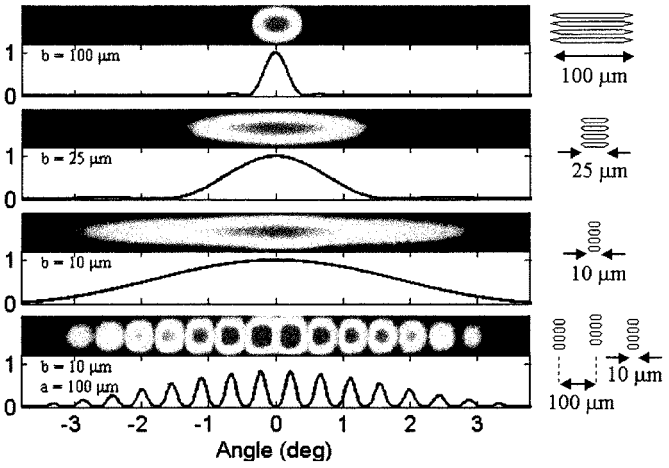

Fig. 3. CCD images and theoretical prediction of far-field diffraction patterns from single slits and a three-slit device (slit width b, center-to-center slit spacing a). The grating pattern for each device is shown schematically on the right. Note that in the shading scheme used for these CCD images, the highest and lowest intensity points appear black unless printed in color.

with 100 mW of average power (1.3-nJ pulses). Devices were heated to 120 °C to avoid any possibility of photorefractive damage. With a loosely focused input beam (140-μm waist), the grating stripes served as 1-D hard apertures, producing SH output with familiar far-field diffraction patterns (Fig. 3). Silicon CCD camera images comparing the measured and expected angular intensity distribution of the SH show excellent agreement for single slit devices (slit widths $b = 100$, 25, and 10 μm), and a three-slit device (slit width $b = 10$ μm, center-to-center slit spacing $a = 100$ μm, π-phase shift on the central slit). The expected intensity distributions can be calculated analytically [6]. Note, that in the shading scheme used for these CCD images, the highest and lowest intensity points appear black unless printed in color.

To investigate phase control between grating stripes, we tested a series of two-slit devices ($b = 10$ μm, $a = 50$ μm) with relative grating phases between 0 and $3\pi/2$. As shown in the calculated intensity distributions and their corresponding CCD images (Fig. 4), adjusting the phase of one slit shifts the far-field (Fraunhofer) diffraction pattern; a π-phase shift produces a complementary distribution of intensity peaks. The 5-mm gratings used in these QPM diffraction demonstrations were long enough that significant diffraction occurs within the device for the smallest grating widths. However, the effect of this finite device length on the far-field angular distribution—of primary interest here—was negligible.

As a simple multiple-slit device demonstration, we periodically poled linear phase arrays of grating stripes for beam steering experiments. These arrays had transverse domain periods of either 16 or 20 μm, extending over 1 mm. A fixed offset (d) between each grating stripe in an array produced a stepwise approximation to a linearly increasing phase front across the SH output beam. In the course of mask fabrication,

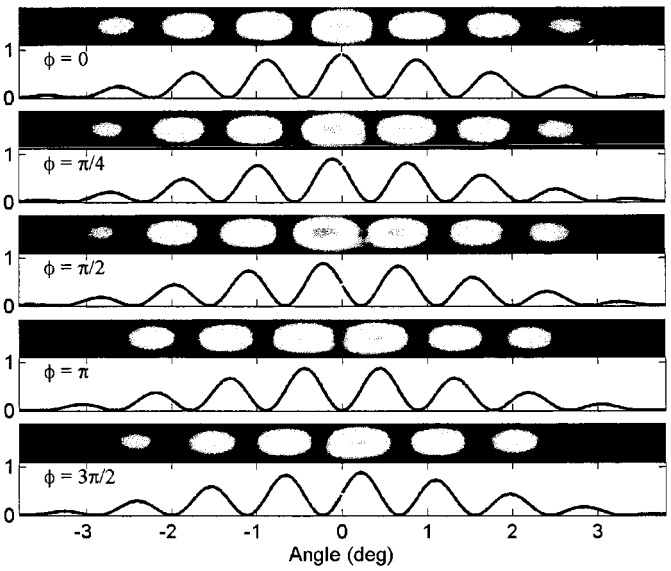

Fig. 4. CCD images and calculated Fraunhofer diffraction from two slits with various relative phases ϕ. A relative displacement d between two gratings results in a relative phase is $\phi = 2\pi d/\Lambda_g$.

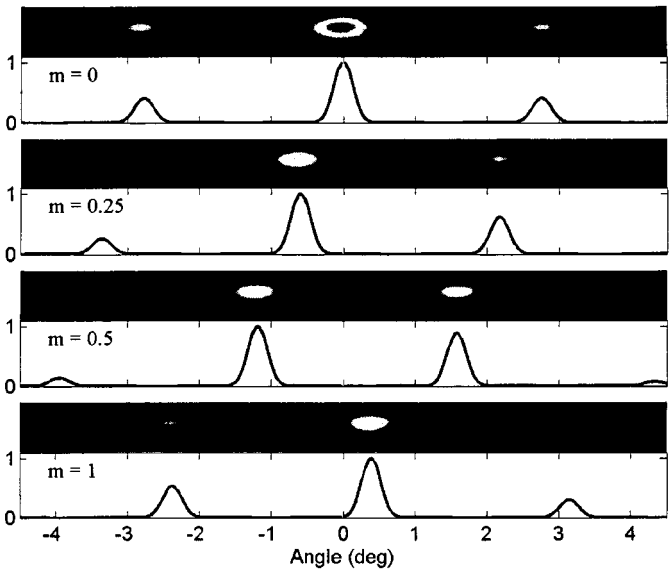

Fig. 5. Measurements and predicted beam steering behavior for linear phase arrays of grating stripes with a variety of phase slopes m.

this constant phase slope was parameterized as a geometric slope m between domain centers; for example, with a 20-μm transverse domain period, a slope $m = 0.5$ corresponded to a domain offset $d = 10$ μm. The phase slope (approximated in discrete steps set by the transverse grating period) for this case, ϕ/20 μm $= 0.054\pi/\mu$m, is representative of the rather large slopes that can be obtained by fine transverse patterning of QPM gratings. Devices with geometric phase slopes between 0 and 1 showed the expected beam steering behavior, along with multiple diffraction peaks due to the 16-μm transverse grating period (Fig. 5). While measuring the SH output, some of the smaller peaks were obscured by the limited dynamic range of the CCD camera. In a separate device, we poled a 17-mm-wide array with a linearly increasing phase slope (parabolic phase). Since the phase slope varied slowly enough

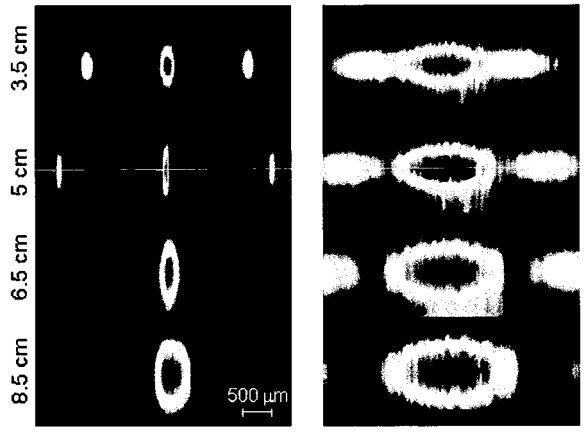

Fig. 6. CCD images of the SH beam at various propagation distances for forward (left column) and backward (right column) transmission through an $f = 5$ cm QPM lens device. Reversing the propagation direction changes the sign of the focal length, a nonreciprocal effect. The 500-μm scale bar applies to all images.

to be treated as constant across the width of the FH beam, we were able to demonstrate a continuously tunable linear phase array by translating the device. As the phase slope was tuned, the far-field intensity peaks shifted in a cyclical fashion; the same intensity pattern appeared each time d increased by an integer multiple of Λ_g because a 2π-phase shift between grating stripes has no effect.

C. QPM Lenses

A transversely patterned array of QPM grating stripes with a parabolic phase profile forms a cylindrical lens for the SH output. The SH output focuses in one dimension only, since the transversely patterned gratings are uniform in depth. We fabricated 5-mm-long QPM lenses with 2-, 5-, and 10-cm focal lengths (f). For each lens the phases of the grating stripes were set by $\phi(r) = kr^2/2f$, where r is the stripe location relative to the lens center and k is the propagation constant at the SH wavelength. To keep the device compact, the displacements (d) needed to set these grating phases were taken modulo Λ_g, as seen in the lens in Fig. 2. The lenses, 1-mm-wide, had a 20-μm transverse grating period (yielding 50 individual grating stripes). With the FH beam expanded to a 600-μm waist, cylindrical focusing of the SH beam was clearly observed by translating a CCD camera along the propagation direction. Fig. 6 shows beam profiles taken at various propagation distances referenced to the end face of a 5-cm focal length lens, confirming the expected waist minimum at 5 cm. As in the linear phase gratings, multiple diffraction orders—which produce multiple foci—result from the periodicity of the transverse patterning.

Measurements of the beam waist versus propagation distance after the QPM lens, taken with a scanning knife-edge beam profiling system, showed nearly ideal focusing behavior. In Fig. 7, data for 2-, 5-, and 10-cm focal length lenses (diamond, square, and circle markers) very closely matches the expected beam propagation, including the calculated minimum waist sizes and locations. The dashed and solid lines are calculations based on an ideal thin lens approximation, and a Green's function approach for the entire grating array [7], respectively. The Green's

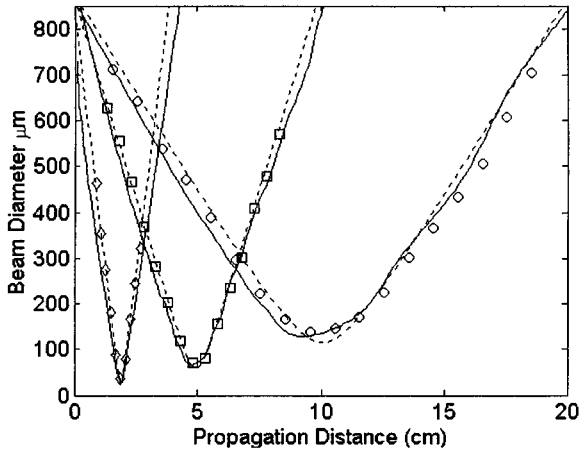

Fig. 7. Measurements (open markers) and calculations of beam waist versus propagation distance for an $f = 5$ cm QPM lens showing good agreement for a thin lens approximation (dashed line), and a calculation using a Green's function approach (solid line).

function calculation integrates the contribution to the nonlinear polarization from each inverted domain, for one output point at a time. Both QPM lens calculations rely only on measurements of the beam profile in front of the sample and have no fitting parameters. Some of the ripples in the beam diameter measurement and calculation result from the slightly non-Gaussian SH beam profile formed by clipping of the expanded FH beam at the edges of the grating array. This clipping could be remedied by making larger QPM lenses, or by varying the grating length or duty cycle to apodize their amplitude profile across the FH beam. The diffracted orders also complicate near-field beam measurements because of interference with the central order; the proper choice of transverse grating pattern could steer these orders farther away, or rearrange their angular distribution more favorably. For the Fresnel amplitude and phase plates, short focal lengths (necessitated by lithographic constraints on the minimum domain size and spacing) combined with inherently low efficiency to prevent decisive characterization.

Although QPM lenses based on SHG are capable of focusing Gaussian beams, they do not have the same imaging properties as conventional lenses because mixing between k vectors in the object wavefront can cause image distortion. However, imaging should be possible with QPM lenses based on sum or difference-frequency-generation (SFG or DFG), using a collimated pump that fills the lens aperture. In this configuration, k vectors in the object wavefront only mix with pump k vectors.

Nonreciprocity is a remarkable feature of QPM lenses. Viewed from the opposite propagation direction, the phase curvature of a parabolic grating array changes sign so that a focal length f becomes $-f$. Turning the device around changes a converging lens into a diverging lens. The two halves of Fig. 6 clearly demonstrate this nonlinear effect, comparing the SH beam at selected distances for forward and backward transmission through a 5-cm focal length QPM lens. After backward transmission through the device, the diverging lens increases beam size and overlap between the diffracted orders. Note that the angular separation of the diffracted orders—the same for forward and backward transmission—can be used to reference CCD image pairs.

Parabolic phase grating arrays and nonphase-shifted grating arrays had the same SHG efficiency. This confirms that adding phase structure to grating arrays does not degrade their amplitude, so that arbitrary phase profiles can be programmed. At the QPM lens output we measured 260 μW of SH output with 100 mW of FH ($\sim$0.21%/nJ efficiency)—a good result given the 5-mm grating length, expanded beam, and 50% transverse grating duty cycle.

III. Conclusion

Transverse patterning of QPM gratings provides a convenient tool for beam shaping, particularly when large phase shifts are required over small spatial scales. While a narrow grating stripe forms a nearly ideal 1-D slit source, phased arrays of grating stripes allow precise tailoring of the amplitude and phase profile of the SH beam. We have demonstrated single and multiple-slit gratings, linear phase arrays, and lenses. This general transverse patterning technique offers many possibilities for other devices, such as beam splitters and combiners. Active devices in which one beam modifies the spatial amplitude or phase profile of another—in a time-gated fashion, if desired—can be designed using SFG or DFG. Chromatic dispersion (both spatial and temporal) can be engineered with multiple grating periods or aperiodic gratings in the transverse or longitudinal directions. QPM lenses might substitute for conventional lenses in some systems, and may be useful for achieving high numerical apertures since their phase profile can be enlarged and tailored with lithographic precision. Their nonreciprocal property could be used for separate manipulation of forward and backward waves in intracavity devices. QPM physical optics structures may both simplify and expand the use of nonlinear optical devices.

References

[1] Y. Ishigame, T. Suhara, and H. Nishihara, "$LiNbO_3$ waveguide second-harmonic-generation device phase matched with a fan-out domain-inverted grating," *Opt. Lett.*, vol. 16, no. 6, pp. 375–377, 1991.

[2] G. Imeshev, M. Proctor, and M. M. Fejer, "Lateral patterning of nonlinear frequency conversion with transversely varying quasiphase-matching gratings," *Opt. Lett.*, vol. 23, no. 9, pp. 673–675, 1998.

[3] V. Berger, "Nonlinear photonic crystals," *Phys. Rev. Lett.*, vol. 81, no. 9, pp. 4136–4139, 1998.

[4] N. G. R. Broderick, G. W. Ross, H. L. Offerhaus, D. J. Richardson, and D. C. Hanna, "Hexagonally poled lithium niobate: A two-dimensional nonlinear photonic crystal," *Phys. Rev. Lett.*, vol. 84, no. 19, pp. 4345–4348, 2000.

[5] G. D. Miller, R. G. Batchko, W. M. Tulloch, D. R. Weise, M. M. Fejer, and R. L. Byer, "42%-efficient single-pass cw second-harmonic generation in periodically poled lithium niobate," *Opt. Lett.*, vol. 22, no. 24, pp. 1834–1836, December 1997.

[6] E. Hecht, *Optics*, Second ed. Redding, MA: Addison-Wesley, 1987.

[7] G. D. Boyd and D. A. Kleinman, "Parametric interaction of focused Gaussian light beams," *J. Appl. Phys.*, vol. 39, no. 8, pp. 3597–3639, 1968.

Jonathan R. Kurz was born in Brooklyn, NY. He received the B.A. degree in physics from Princeton University. Princeton, NJ, and the M.S. degree in applied physics from Stanford University, Stanford, CA, in 1997 and 1999, respectively. He is working towards the Ph.D. degree, studying guided wave nonlinear optical devices.

Andrew M. Schober was born in Avon, OH, in 1976. He received the B.S. degree in physics from Case Western Reserve University, Cleveland, OH, and the M.S. degree in applied physics from Stanford University, Stanford, CA, in 1998 and 2001, respectively. He is working toward the Ph.D. degree in applied physics at Stanford University.

David S. Hum was born in Ottawa, Canada in 1977. He received the B.A.Sc. degree in electrical engineering from the University of Toronto, Toronto, Canada, in 2000. He is working toward the Ph.D. degree at Stanford University, Stanford, CA, in electrical engineering.

A. J. Saltzman, photograph and biography were not available at the time of publication.

Martin M. Fejer (M'93) received the B.A. degree in physics from Cornell University, and the Ph.D. in applied physics from Stanford University, Stanford, CA, in 1986.

In 1986, he joined the faculty at Stanford, where he is currently a professor of applied physics. With more than a dozen students and postdoctoral researchers, his research group focuses on nonlinear optical materials and devices, guided wave optics, microstructured ferroelectrics and semiconductors, nonlinear devices for telecom applications, low dissipation materials, and precision measurements. He has served as the program committee chair and general chair for numerous technical meetings, including the Advanced Solid-State Lasers Topical Meeting, the Conference on Lasers and Electro-Optics, the Nonlinear Guided Wave Optics Topical Meeting, and the Integrated Photonics Research Meeting. In 1998, he received the R. W. Wood Prize. He has authored over 180 technical publications and holds 17 patents.

He is a fellow of the Optical Society of America and currently chairs the Quantum Electronics Division, and is a member of the American Physical Society, America Society for the Crystal Growth, and The International Society for Optical Engineering.